Application of NaOH-treated rice husk for adsorptive discharge of cobalt ions from wastewater

Shagufta Zafar[a,b,†], Muhammad Imran Khan[c,*,†], Warda Hassan[d], Sidra Mubeen[d], Tariq Javed[e], Shabnam Shahida[f], Suryyia Manzoor[g,*], Abdallah Shanableh[c], Aziz ur Rehman[b], Muhammad Latif Mirza[b], Nasir Khalid[h], Mushtaq Hussain Lashari[i,*]

[a]Department of Chemistry, The Government Sadiq College Women University, Bahawalpur 63000, Pakistan, email: shg_zf@gscwu.edu.pk
[b]Department of Chemistry, The Islamia University of Bahawalpur, Bahawalpur, Pakistan, emails: azizypk@yahoo.com (A. ur Rehman), mlatifmirza@gmail.com (M.L. Mirza)
[c]Research Institute of Sciences and Engineering, University of Sharjah, Sharjah 27272, United Arab Emirates, emails: raoimranishaq@gmail.com (M.I. Khan), shanableh@sharjah.ac.ae (A. Shanableh)
[d]Department of Chemistry, The Women University Multan, Katchery Campus, LMQ Road, Multan, emails: warda.chem@wum.edu.pk (W. Hassan), sidra_sidra786@yahoo.com (S. Mubeen)
[e]Department of Chemistry, University of Sahiwal, Sahiwal, Pakistan, email: jtariq56@yahoo.com
[f]Department of Chemistry, University of Poonch, Rawalakot 12350, Azad Kashmir, Pakistan, email: shabnamshahida01@gmail.com
[g]Institute of Chemical Sciences, Bahauddin Zakariya University, Multan 60800, Pakistan, email: suryyia.manzoor@bzu.edu.pk
[h]Chemistry Division, Pakistan Institute of Nuclear Science and Technology, PO Nilore, Islamabad, Pakistan, email: mkhalid@gmail.com
[i]Department of Zoology, The Islamia University of Bahawalpur, Bahawalpur 63100, Pakistan, email: mushtaqlashary@gmail.com

A B S T R A C T

In this research, batch adsorption of cobalt ions (Co(II)) from wastewater onto NaOH-treated rice husk (TRH) was studied at room temperature. Several techniques such as Fourier transform infrared, scanning electron microscopy, and energy diffraction X-rays were used to prove adsorption of Co(II) onto TRH. The percentage discharge of Co(II) was increased with the contact time, amount of TRH, and temperature whereas decreased with an initial concentration of Co(II) solution. Nonlinear isotherms such as Langmuir, Freundlich, and Dubinin–Radushkevich were utilized to study experimental data for adsorption of Co(II) onto TRH. Results showed that experimental data fitted well to nonlinear isotherms. The value of Langmuir constant Q_m was 9.35×10^{-5} mol/g. Adsorption kinetics was studied by using pseudo-first-order model, pseudo-second-order model, Elovich model, liquid film diffusion model, modified Freundlich equation, and Bangham equation. Results exhibited that experimental data for adsorption of Co(II) fitted well to pseudo-second-order model having k_2 numerical value of 0.45 g/mg min. Thermodynamic analysis revealed that adsorption of Co(II) from wastewater was endothermic with a change in enthalpy ($\Delta H°$) value of 15.406 kJ/mol and spontaneous process. Desorption of Co(II) from TRH was also investigated. Hence, TRH could be used as an excellent adsorbent for the discharge of Co(II) from wastewater.

Keywords: Treated rice husk; Nonlinear isotherms; Adsorption; Endothermic process; Cobalt ions

---

* Corresponding author.

†Both authors contributed equally to this work.

1. Introduction

Usually, heavy metals are hazardous to the environment and organisms because of their inherent toxicity and the ability to assemble in living tissues [1]. They can cause several issues for the animals and human's health as well as the environment [2,3]. Cobalt ion is crucial for metabolic activities in low concentrations and may also be efficient in regulating pro-oxidants in the blood [4–6]. After all, in high concentrations, it results in acute influences of lung toxicity and asthma, inflammation of the lungs, and chest tightness [7,8]. The International Agency for Research on Cancer (IARC), has described cobalt as a probable carcinogen. By EPA, the maximum level of cobalt in drinking water was approved to be 40 µg/L [9]. Industrial wastewater is the cause of water pollution due to heavy metals. The discharge of these pollutants before the removal of wastewater into the environment is crucial in view of public health and pollution control [9].

A lot of traditional processes including chemical precipitation [10], ion exchange [11], flotation [12], coagulation [13], membrane processes [14], solvent extraction [15], and adsorption [16–18] were developed to remove heavy metals from aqueous solutions. Adsorption is a significant process to discharge heavy metals. Adsorption has a lot of benefits namely easy operation, high efficiency, low cost, and production of less sludge volume [19]. Several kinds of materials including activated carbons [20], carbon nanotubes [21], nanosponge biopolymer [22], zeolites [23], chitosan [24], clays [25], and agricultural wastes [3] were investigated to discharge metal cations from aqueous solutions.

In our previous research, we used leaves the power of different plants [26–29] and anion exchange membranes [30,31] for discharge of dyes from wastewater. We also used rice husk to discharge metal ions from an aqueous solution [32,33]. In this manuscript, NaOH-treated rice husk (TRH) was employed for the removal of Co(II) from wastewater at ambient temperature to extend our research. The effect of operating factors on the adsorption of Co(II) onto TRH was also investigated. Adsorption kinetics, isotherms, and thermodynamics were revealed in detail. The recovery of Co(II) and regeneration of TRH was also studied.

2. Experimental

2.1. Materials

Herein, all the chemicals utilized were of analytical grade and used as received. The temperature of the solution was controlled by soaking the culture tube in the water bath of Gallen Kamp thermo stirrer (UK) for thermodynamic investigations. The fidelity of the temperature in the water bath was ±0.1°C. Deionized water was utilized throughout the research.

2.2. Adsorbent

Husk of basmati rice was provided by a rice mill in the Punjab Province of Pakistan. To withdraw dust particle, the samples were thoroughly cleaned and were oven-dried at 80°C till constant weight was achieved. The washed and dried rice husk was treated with 1.0 M NaOH. In the NaOH solution, 500 g of rice husk was added to a 2 L beaker. The mixture was stirred vigorously and the whole mixture was heated at 60°C for 2 h. The contents were left overnight at room temperature. After that, the rice husk was washed with water until the neutral pH of the washing was attained. The adsorbent was dried in the oven at 80°C till constant weight and stored in an airtight container and labeled as TRH. Neutron activation analysis (NAA) and atomic adsorption spectrometry (AAS) methods were utilized for the chemical analysis of husk samples for their trace metal contents and attained results were reported [33,34]. These results showed that the quantity of metals such as Na, K, Pb, and Fe were present in µg per g of sample. Silica contents were found to be 18.27 (0.62%) of TRH. The trace quantity of elements present in TRH was studied by utilizing standard procedures.

2.3. Adsorption test

Adsorption test was carried out as reported in our previous work [32,33,35,36]. In a typical procedure, a known amount of TRH was taken into a 25 cm^3 secured cap culture tube along with 4 cm^3 of standard acid solution, and a fixed quantity of stock radiotracer with a known quantity of Co(II) solution was added. Consecutively, the contents were equilibrated on a wrist-action mechanical shaker (Vibromatic (USA)) at a rate of 500 rpm for specific intervals of time. Then, it was centrifuged at 5,000 rpm for phase separation and the supernatant solution was withdrawn for activity measurement. The radioactivity of solutions before (A_i) and after (A_f) equilibrium was recorded with a NaI well-type scintillation counter (Canberra Inc., United States) coupled with a counter-scaler (Nuclear Chicago). A volume of 1.0 cm^3 was normally used to measure the activity. All experiments were performed at ambient temperature. The percentage adsorption of Co(II) onto TRH was calculated by utilizing the below equation:

$$\% \text{ adsorption} = \frac{A_i - A_f}{A_i} \times 100 \tag{1}$$

where A_i and A_f denote initial and final adsorption of Co(II) (counts/min) into, respectively.

Desorption of Co(II) was carried out by immersing a specific quantity of Co(II) loaded TRH into an aqueous solution of HNO_3 (0.1 mol/L) as a desorbing media for a specific time as reported in our previous work [36].

2.4. Characterization

2.4.1. Instrumentation

Fourier transforms infrared (FTIR) spectrum of TRH before and after adsorption of Co(II) was recorded by utilizing attenuated total reflectance (ATR) with FTIR spectrometer (Vector 22, Bruker) having a resolution of 2 cm^{-1} and total spectral range of 4,000–400 cm^{-1}. The structure of TRH before and after adsorption of Co(II) was studied by field emission scanning electron microscopy (FE-SEM, Sirion200, FEI Company, USA). Energy dispersive X-ray (EDX) analysis was employed to study the adsorption of Co(II) onto TRH.

2.5. Nonlinear adsorption isotherms

Experimental data for adsorption of Co(II) onto TRH was subjected to different nonlinear adsorption isotherms which are as follows:

Nonlinear Langmuir adsorption isotherm is shown as [36]:

$$C_{ads} = \frac{Q_m k_L C_e}{1 + k_L C_e}$$ (2)

where C_e is the concentration of Co(II) solution (mol/L) at equilibrium. The constant Q_m is monolayer adsorption capacity (mol/g) and K_L (L/mol) is related to the energy of adsorption. In general Q_m and K_L are functions of pH, ionic media, and ionic strength.

Nonlinear Freundlich isotherm is represented as [36]:

$$C_{ads} = K_f C_e^{1/n}$$ (3)

where "K_f" and "n" are Freundlich constants denoting adsorption capacity and adsorption intensity respectively.

Nonlinear D–R equation can be given as [32]:

$$C_{ads} = C_m \exp\left(-\beta \varepsilon^2\right)$$ (4)

where C_{ads} is the quantity of Co(II) adsorbed onto TRH, C_m (mol/g) is the maximum quantity of Co(II) that can be adsorbed onto TRH under the optimized experimental conditions, β is a constant related to adsorption energy and ε (Polyanyi potential) = $RT\ln(1 + 1/C_e)$ where R is the universal gas constant (kJ/mol K), and T is the absolute temperature (K).

The mean adsorption energy (E) can be calculated by utilizing the value of β as [32]:

$$E = \frac{1}{\sqrt{2\beta}}$$ (5)

2.6. Adsorption kinetics

Several adsorption models were utilized to investigate the controlling mechanism of the adsorption process such as chemical reaction and diffusion control.

2.6.1. Pseudo-first-order model

The linearized form of the Lagergren pseudo-first-order rate equation is represented as [37,38]:

$$\log(q_e - q_t) = \log q_e - \frac{K_1 t}{2.303}$$ (6)

where q_e and q_t show the adsorbed amount of Co(II) at equilibrium and time t respectively and k_1 (/min) is the rate constant of the pseudo-first-order model.

2.6.2. Pseudo-second-order model

The linearized form of the pseudo-second-order kinetic model is shown as [39]:

$$\frac{t}{q_t} = \frac{1}{k_2 q_e^2} + \frac{t}{q_e}$$ (7)

where k_2 (g/mg min) is the rate constant of the pseudo-second-order model.

2.6.3. Elovich model

The most interesting model to explain the activated chemisorption is the Elovich model [32]:

$$q_t = \frac{1}{\beta}\ln(\alpha\beta) + \frac{1}{\beta}\ln t$$ (8)

where α (mg/g min) and β (g/mg) are constant. The parameter α is considered as initial adsorption rate (mg/g min) and β is related to the extent of surface coverage and activation energy for chemisorption.

2.6.4. Liquid film diffusion model

The liquid film diffusion model is given as [32,37]:

$$\ln\left(1 - \frac{q_t}{q_e}\right) = -K_{fd} t$$ (9)

where K_{fd} shows liquid film diffusion rate constant.

2.6.5. Modified Freundlich equation

The modified Freundlich equation was originally developed by Kuo and Lotse [38]:

$$q_t = kC_0 t^{1/m}$$ (10)

where k shows the apparent adsorption rate constant (L/g min), C_0 depicts the initial concentration (mg/L) of Co(II) solution, t shows the contact time (min), and m represents the Kuo–Lotse constant. The values of k and m were utilized to investigate the influence of Co(II) surface loading and ionic strength on the adsorption process. A linear form of modified Freundlich equation is expressed as:

$$\ln q_t = \ln\left(kC_0\right) + \frac{1}{m}\ln t$$ (11)

2.6.6. Bangham equation

Bangham equation is expressed as [40]:

$$\log\log\left(\frac{C_0}{C_0 - q_t m}\right) = \log\left(\frac{k_0 m}{2.303 V}\right) + \alpha \log t$$ (12)

where V is the volume of solution (mL), m is the weight of adsorbent used (g/L). α (<1) and k_0 (mL/(g/L)) are constants.

2.7. Thermodynamics study

Thermodynamics for adsorption of Co(II) onto TRH was also evaluated. The values of change in Gibb's free energy ($\Delta G°$), enthalpy ($\Delta H°$), and entropy ($\Delta S°$) were determined by using the below equations:

$$\ln K_c = \frac{\Delta S°}{R} - \frac{\Delta H°}{RT} \tag{13}$$

$$K_c = \frac{C_a}{C_e} \tag{14}$$

$$\Delta G° = \Delta H° - T\Delta S° \tag{15}$$

where K_c, $\Delta G°$, $\Delta H°$, and $\Delta S°$ are equilibrium constant, change in Gibb's free energy (kJ/mol), enthalpy (kJ/mol), and entropy (J/mol K), respectively.

3. Results and discussion

3.1. FTIR test

Fig. S1 represents the FTIR spectrum of virgin TRH. The peaks at 1,737.8; 1,435.6; and 1,365.4 cm^{-1} were attributed to C=O stretching, OH bending of the adsorbed H$_2$O, and aliphatic C–H bending, respectively [41]. The peak at 3,400–3,200 cm^{-1} was due to the surface O–H stretching, whereas aliphatic C–H stretching had broadband at 2,921–2,851 cm^{-1}. The peaks at 1,217.0; 1,365.4; 1,737.8; and 1,027.4 cm^{-1} were due to the carboxyl group on TRH in the range of reported peaks at 1,208–1,230; 1,367–1,371; 1,740 and 1,029 cm^{-1} for carboxyl group [42,43]. Except, the peak at 1,074.0 cm^{-1} coincides with the anti–symmetric stretching vibration of Si–O, whereas at 476.2 cm^{-1} showed the bending vibration of Si–O–Si bond [42,44,45]. The lack of peaks related to non–conjugated carbonyl functional groups in the TRH spectrum represented hydrolyses of carbonyl groups during NaOH treatment.

Fig. S1 indicates the FTIR spectrum of TRH after adsorption Co(II). The changes observed in the spectrum of Co(II) loaded TRH were the slight shifts of 1,739.4 and 1,367.3 cm^{-1} peak of carbonyl, carboxyl functional groups and a decrease in their intensities were observed. A shift of ~12 and 11 cm^{-1} was seen in 1,217.0 and 1,029 cm^{-1} peak. It suggested the involvement of these functional groups in Co(II) adsorption onto TRH. Similar results were reported in the literature for the adsorption of cobalt ions on lignocellulose/montmorillonite nanocomposite [46].

3.2. Scanning electron microscopy and energy-dispersive X-ray tests

The structure of TRH before and after adsorption of Co(II) was investigated by using scanning electron microscopy (SEM). SEM images of virgin and Co(II) loaded TRH are represented in Fig. S2. Results showed that the surface roughness of TRH was changed significantly after Co(II) adsorption. The surface of the adsorbent became smooth because of Co(II) adsorption. The pores present onto TRH were much greater in size than the ionic radius of cobalt (0.088 nm) which supported its adsorption into the pores of TRH. The adsorption capacity was enhanced from 1.385×10^{-5} to 1.05×10^{-4} mol/g for Co(II) because of the creation of more active sites of TRH

EDX test of Co(II) loaded TRH was utilized to determine the presence of Co(II) onto TRH. EDX image of Co(II) loaded TRH is shown in Fig. S3. The metal ion peaks located at different energy levels ranging 0.550–7.650 keV represented its adsorption onto TRH.

3.3. Effect of operating factors

The effect of operating factors such as contact time, amount of TRH, initial concentration of Co(II) solution, and temperature on the percentage removal of Co(II) was studied. The details are reported below.

3.3.1. Effect of contact time

It was elucidated keeping amount TRH, shaking speed, initial concentration of Co(II) solution, temperature, and volume of solution constant, and attained results are shown in Fig. 1a. The percentage removal of Co(II) from wastewater by using TRH was increased with contact time. It was enhanced from 74% to 98.50% with contact time at room temperature. It was higher than untreated rice husk [36]. In the start, the removal of Co(II) from wastewater was very fast due to the presence of a large number of vacant sites onto TRH and interaction was developed between Co(II) and adsorption sites. Then, there was no large increase in the removal of Co(II) after this equilibrium was reached and no further crucial increase in adsorption was achieved with contact time. It slowed down due to the movement of Co(II) into the interior pores of TRH when all surface sites were occupied.

3.3.2. Effect of amount of TRH

The effect of the amount of TRH was studied keeping other operating factors constant at room temperature. Fig. 1b depicts the effect of the amount of TRH on the percentage discharge of Co(II) from wastewater at ambient temperature. It was enhanced from 37% to 98.50% with enhancing amount of TRH. The optimized amount of TRH was 0.10 g because after this the variation in the percentage removal of Co(II) from wastewater was small. Therefore, it was utilized in further studies.

3.3.3. Effect of initial concentration of Co(II) solution

The effect of initial concentration of Co(II) onto the percentage removal of Co(II) from wastewater was investigated keeping other operating endowments constant at ambient temperature and results are shown in Fig. 1c. Results showed that the percentage removal of Co(II) from wastewater was decreased with enhancing the initial concentration of Co(II)
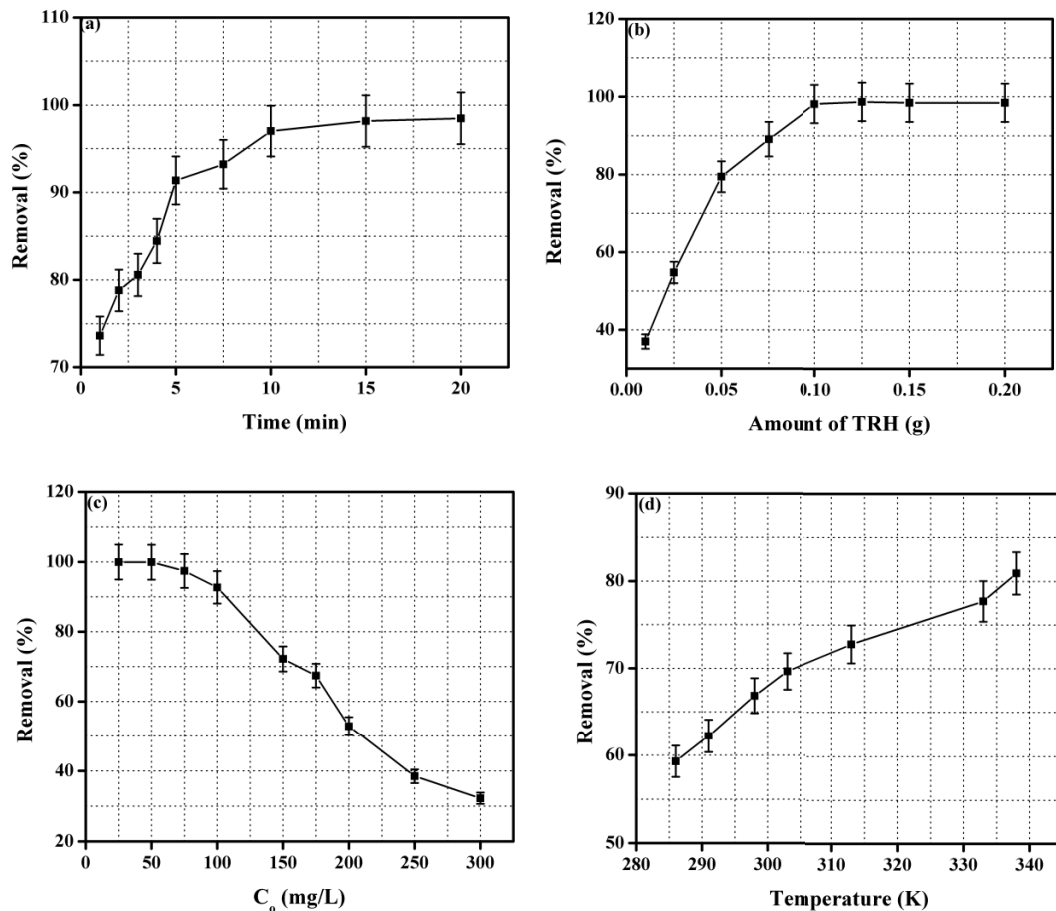
Fig. 1. (a) Effect of contact time, (b) amount of TRH, (c) initial concentration of Co(II) solution, and (d) temperature on the percentage removal of Co(II) from aqueous solution.

at room temperature. At higher initial concentrations, some of Co(II) were left unabsorbed due to saturation of adsorption spaces. More binding spaces existed at a low concentration of metal ions. The number of ions competing for present binding spaces onto TRH was increased with enhancing concentration on metal ions.

3.3.4. Effect of temperature

Fig. 1d represents the effect of temperature on the removal of Co(II) from wastewater by utilizing TRH as an adsorbent. It was studied keeping other operating factors constant. It was found that the percentage removal of Co(II) was increased from 61% to 81% with temperature rise. The increase in adsorption of Co(II) may be either due to the acceleration of some initially slow adsorption stages or to the establishment of some new active spaces onto the surface of the TRH with the rise in temperature [32,36].

3.4. Adsorption isotherms

Fig. 2 depicts Langmuir isotherm for adsorption of Co(II) onto TRH. Wavemetrices IGOR Pro 6.1.2 software was employed for the calculation of isotherm parameters by utilizing nonlinear equations and attained values are given
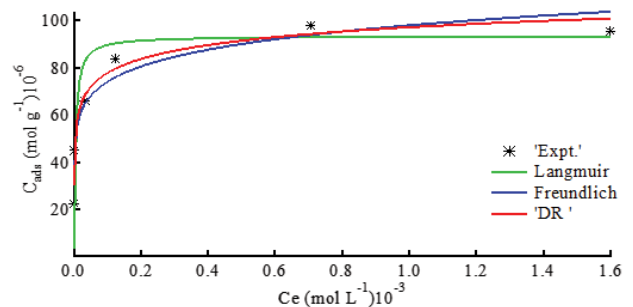

Fig. 2. Nonlinear plots of Langmuir, Freundlich, and D–R isotherms for adsorption of Co(II) onto TRH.

in Table 1. For adsorption of Co(II) onto TRH, the values of R_L were calculated from Langmuir constant K_L and initial concentrations of Co(II) and are given in Table 1 which showed that adsorption of Co(II) was the favorable process.

Fig. 2 represents Freundlich isotherm for adsorption of Co(II) onto TRH and determined values of K_f and n are given in Table 1. The value of n was utilized to signify the heterogeneous surface of the TRH (adsorbent). The values of "n" ranges from 2 to 10 indicating good adsorption, 1–2

Table 1
Determined parameters of Langmuir, Freundlich, and Dubinin–Radushkevivh (D–R) isotherms by nonlinear method

Adsorption isotherms	Isotherm parameters	
Langmuir isotherm	Q_m	9.35×10^{-5}
	K_L	235,150
	R_L	0.001–0.010
	χ^2	1.76×10^{-9}
Freundlich isotherm	K_f	$2.27 \times 10^{-4} \pm 3.95 \times 10^{-5}$
	n	8.240 ± 1.36
	χ^2	3.00×10^{-10}
Dubinin–Radushkevich (D–R) isotherm	C_m	$(1.300 \pm 0.086) \times 10^{-4}$
	B	$(9.900 \pm 1.26) \times 10^{-4}$
	E	22.43 ± 2.85
	χ^2	1.60×10^{-10}

Q_m: mol/g; K_L: L/mol; K_f: (mg/g) (L/mg)$^{1/n}$; C_m: mol/g; β: mol^2/J^2; E: kJ/mol

Table 2
Adsorption capacities of cobalt for different adsorbents

Adsorbent	Capacity (mg/g)	References
Chitosan coated perlite beads	1.406	[48]
Coir pith	7.29	[49]
Bentonite	4.95	[50]
Crab shell	0.92	[51]
Chitosan coated perlite beads	1.208	[52]
Sheep manure	0.5759	[54]
Modified sheep manure	1.085	[54]
Arca shell	2.853	[55]
Rice husk	2.500	[56]
Natural bentonite	3.834	[57]
Treated rice husk	19.203	Present study

moderate adsorption, and less than one represents poor adsorption [36,47]. The determined adsorption capacity of cobalt ion on TRH was compared with the reported values for different adsorbents and the results are shown in Table 2. The determined adsorption capacity values for rice husk were significantly higher than coir pith, arca shell, and bentonite whereas it is much higher than chitosan-coated perlite beads, crab shells, and modified and simple sheep manure.

Fig. 2 shows D–R isotherm for adsorption of Co(II) onto TRH. The values D–R constants were calculated by utilizing a computer program Wavemetrices Igor Pro 6.2.1.2 and are given in Table 1 along with their respective (χ^2) values which can be used as a best-fitting tool in the nonlinear method. Low numerical values of "χ^2" for nonlinear isotherms represent that experimental data fitted well to D-R isotherm. The value of adsorption-free energy (E) was 22.43 ± 2.85 kJ/

mol. It showed that adsorption of Co(II) onto TRH was a physical adsorption process.

3.5. Adsorption kinetics study

The plot of pseudo-first-order for adsorption of Co(II) onto TRH is represented in Fig. 3a. The determined values of k_1 and q_e from slope and intercept of the plot are given in Table 3. The value of the correlation coefficient (R^2) was 0.980. Further, there was a large difference between calculated adsorption capacity values ($q_{e,cal}$) and experimental adsorption capacity ($q_{e,exp}$). Therefore, it does not explain the rating process.

Fig. 3b shows the plot of the pseudo-second-order model. The value of adsorption capacity was determined from the slope and is given in Table 3. It was very close to the experimental value (3.525 mg/g). Further, the value of the correlation coefficient was close to unity ($R^2 > 0.999$). It indicated that experimental data fitted well to the pseudo-second-order model.

Fig. 3c shows the plot of the Elovich model. The calculated values of α and β from intercept and slope are given in Table 3. The value of correlation coefficient (R^2) was lower than that of the pseudo-second-order model.

The plot of $\ln(1 - q_t/q_e)$ vs. time for the liquid film diffusion model is depicted in Fig. 3d. The calculated value of K_{fd} from the slope of the linear plot is given in Table 3. The value of the correlation coefficient for the liquid film diffusion model was lower than the pseudo-second-order model. It showed that it cannot be sufficient to explain experimental data.

Fig. 4a indicates the plot of the modified Freundlich equation for adsorption of Co(II) onto TRH. The measured values of m and k from slope and intercept are given in Table 3. The value of the correlation coefficient (R^2) was 0.938. It revealed that experiment data was not fitted to the modified Freundlich equation.

The plot of log-log($C_0/C_0 - q_t m$) vs. log$t$ for Bangham equation is indicated in Fig. 4b. The determined values of α and m are given in Table 3. The double logarithmic plot did not give a linear curve for adsorption of Co(II) denoting that the diffusion of adsorbate into pores of the adsorbent (TRH) is not the only rate-controlling step [36]. It may be that both film and pore diffusion were significant to a different extent in adsorption of Co(II) onto TRH.

3.6. Adsorption thermodynamics

Fig. 4c shows the plot of lnK_c vs. $1/T$ for adsorption of Co(II) onto TRH. The measured values of thermodynamic parameters are given in Table 4. The positive value of enthalpy ($\Delta H°$) revealed that adsorption of Co(II) was an endothermic process. Moreover, the positive value of entropy ($\Delta S°$) exhibited enhancement in randomness at the adsorbent–adsorbate interface during adsorption of Co(II) onto TRH. The negative value of Gibb's free energy indicated that the adsorption process was spontaneous in nature. The decrease in values of Gibb's free energy with temperature rise represented the decline in the feasibility of adsorption at elevated temperatures.
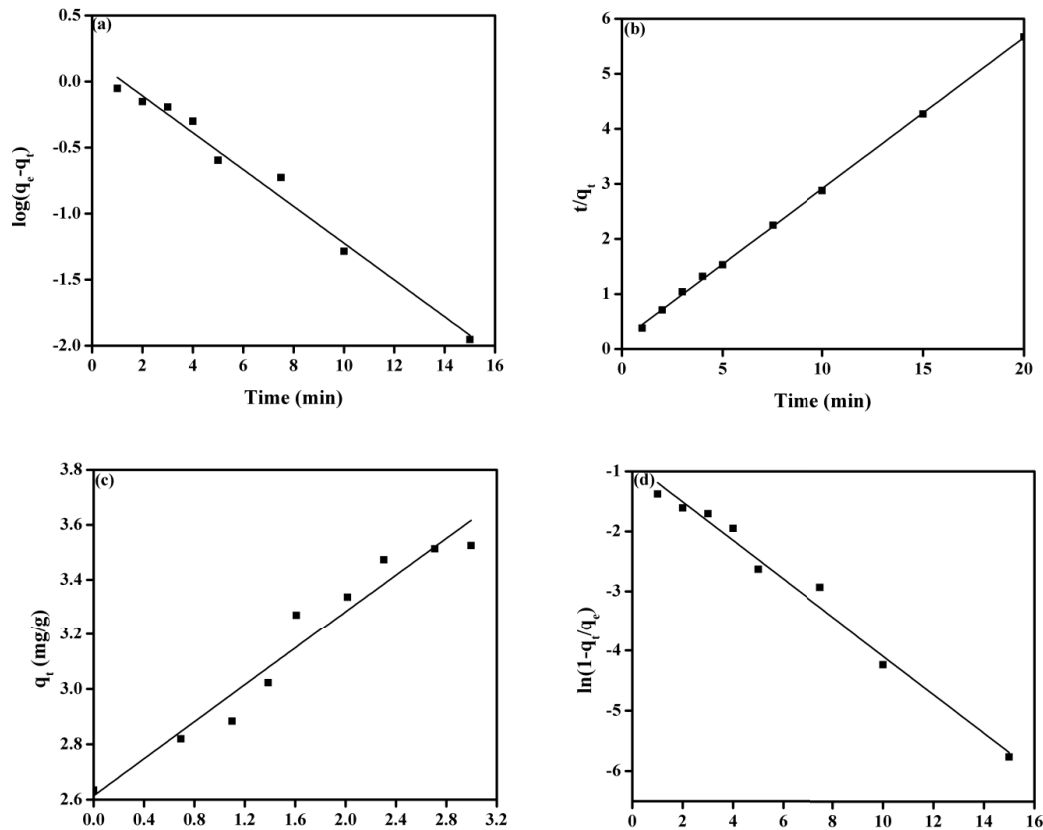
Fig. 3. (a) Pseudo-first-order model, (2) pseudo-second-order model, (c) Elovich model, and (d) liquid film diffusion model for adsorption of Co(II) onto TRH.

Table 3
Calculated parameters of applied kinetic models for adsorption of Co(II) onto TRH

Kinetic models	Parameters	
Pseudo-first-order model	$q_{e,\text{exp}}$	3.525
	q_e	1.48
	$k_1 \times 10^{-2}$	6.10
	R^2	0.980
Pseudo-second-order model	q_e	3.642
	k_2	0.45
	R^2	0.999
Elovich model	A	829
	B	2.99
	R^2	0.940
Liquid film diffusion model	K_{fd}	0.32
	C_{fd}	−0.87
	R^2	0.980
	M	9.27
Modified Freundlich equation	K	0.039
	R^2	0.938
Bangham equation	$k_0 \times 10^{-4}$	1.57
	A	0.11
	R^2	0.938

q_e: mg/g; k_1: (/min); k_2: g/mg min; α: mg/g min; β: g/mg; K_{fd}: (/min); K: L/g min; k_0: mL/g/L

3.7. Recovery of Co(II)

The recovery of Co(II) and regeneration of TRH are important for the wastewater treatment process. Many efforts were made to recover Co(II) from the TRH surface by utilizing HNO_3 as desorbing media. HNO_3 solution of different molarities was used in batch mode. For this, the fixed amount of Co(II) loaded TRH was shaked with HNO_3 for the specific time for recovery of Co(II). Several experiments were performed by varying concentrations of HNO_3 solutions for desorption of Co(II) from TRH. The maximum recovery of Co(II) (~90%) was achieved with 1.0 mol/L HNO_3 solution from TRH within 5 min time.

4. Conclusions

In this manuscript, the adsorptive removal of Co(II) from wastewater by using TRH was evaluated. The removal of Co(II) was increased with the contact time, amount of TRH, and temperature whereas decreased with an initial concentration of Co(II) solution. Equilibrium isotherm results exhibited that experimental data for adsorption of Co(II) onto TRH followed nonlinear Langmuir isotherm model. Adsorption kinetics results revealed that adsorption of Co(II) onto TRH fitted to pseudo-second-order model. Thermodynamic evaluation showed that adsorption of Co(II) onto TRH was endothermic and spontaneous process. Further, the recovery of Co(II) was maximum for
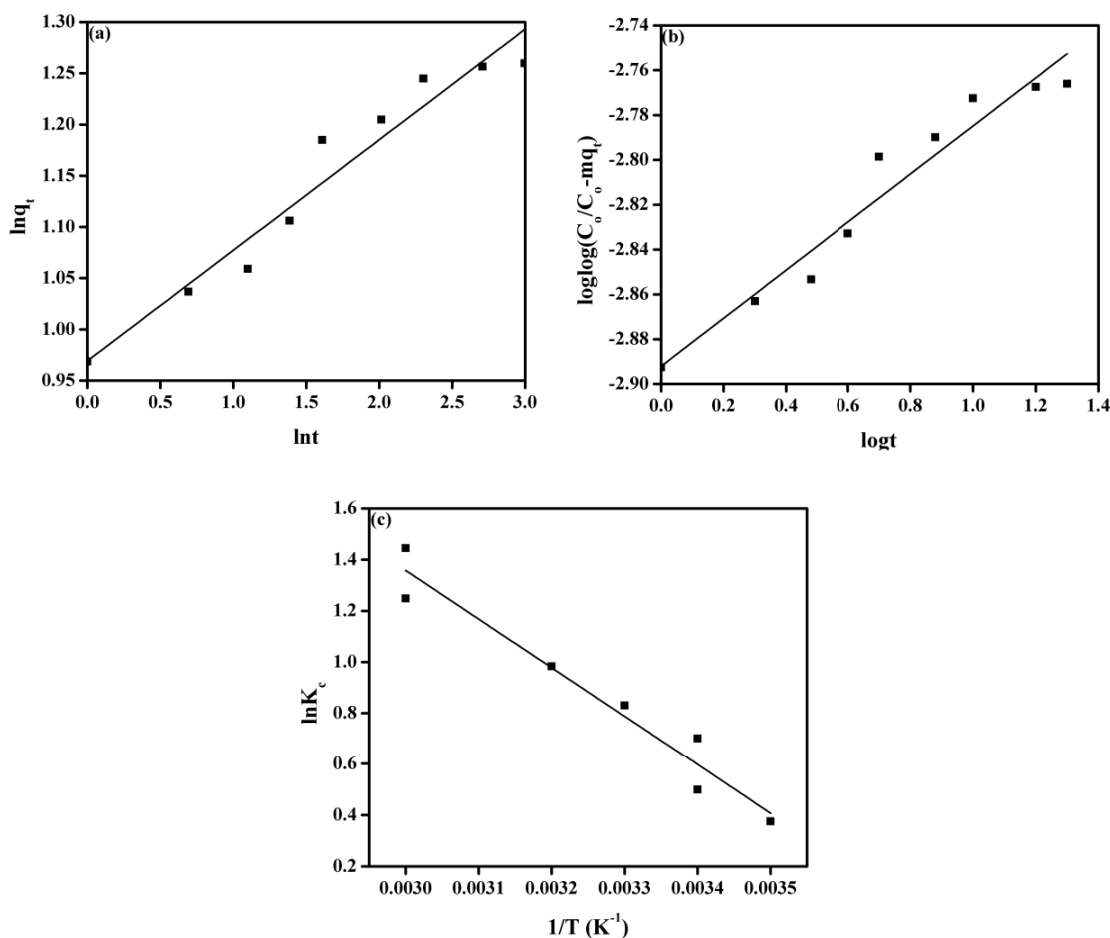
Fig. 4. (a) Modifies Freundlich equation, (2) Bangham equation, and (c) the plot of $1/T$ vs. $\ln K_c$ for adsorption of Co(II) onto TRH.

Table 4
Determined thermodynamic parameters for adsorption of Co(II) onto TRH

Temperature (K)	$\Delta H°$ (kJ/mol)	$\Delta S°$ (J/K mol)	$\Delta G°$ (kJ/mol)
286.16			−0.978
291.16			−1.264
298.16			−1.665
303.16	15.406	57.285	−1.952
313.16			−2.524
333.16			−3.670
338.16			−3.957

HNO_3 (1.0 mol/L) solution. Hence, TRH could be employed as an extraordinary adsorbent for the removal of Co(II) from wastewaters.

Acknowledgments

References

[1] M. Miri, E. Akbari, A. Amrane, S.J. Jafari, H. Eslami, E. Hoseinzadeh, M. Zarrabi, J. Salimi, M. Sayyad-Arbabi, M. Taghavi, Health risk assessment of heavy metal intake due to fish consumption in the Sistan region, Iran, Environ. Monit. Assess., 189 (2017) 1–10.

[2] H. Eslami, M.R. Samaei, E. Shahsavani, A.A. Ebrahimi, Biodegradation and fate of linear alkylbenzene sulfonate in integrated fixed-film activated sludge using synthetic media, Desal. Water Treat., 92 (2017) 128–133.

[3] J.B. Arup Roy, Role of nanotechnology in water treatment and purification: potential applications implications, Sep. Purif. Technol., 115 (2013) 172–179.

[4] M.R. Awual, T. Yaita, Y. Okamoto, A novel ligand based dual conjugate adsorbent for cobalt(II) and copper(II) ions capturing from water, Sens. Actuators, B, 203 (2014) 71–80.

[5] H. Chen, J. Li, D. Shao, X. Ren, X. Wang, Poly(acrylic acid) grafted multiwall carbon nanotubes by plasma techniques for Co(II) removal from aqueous solution, Chem. Eng. J., 210 (2012) 475–481.

[6] X. Li, C. Zeng, J. Jiang, L. Ai, Magnetic cobalt nanoparticles embedded in hierarchically porous nitrogen-doped carbon frameworks for highly efficient and well-recyclable catalysis, J. Mater. Chem. A, 4 (2016) 7476–7482.

[7] M. Abbas, S. Kaddour, M. Trari, Kinetic and equilibrium studies of cobalt adsorption on apricot stone activated carbon, J. Ind. Eng. Chem., 20 (2014) 745–751.

[8] A. Shahat, M.R. Awual, M. Naushad, Functional ligand anchored nanomaterial based facial adsorbent for cobalt(II) detection and removal from water samples, Chem. Eng. J., 271 (2015) 155–163.

[9] M.H. Salmani, M.H. Ehrampoush, H. Eslami, B. Eftekhar, Synthesis, characterization and application of mesoporous silica in removal of cobalt ions from contaminated water, Groundwater Sustainable Dev., 11 (2020) 1–9.

[10] V.V. Goncharuk, B. Kornilovich, V.M. Pavlenko, M.I. Babak, G.N. Pshinko, B.V. Pysmennyi, I. Kovahuk, V.G. Safronava, Uranium compounds purification from water and wastewater, J. Water Chem. Technol., 23 (2001) 44.

[11] F. Ferella, M. Prisciandaro, I. De Michelis, F. Veglio', Removal of heavy metals by surfactant-enhanced ultrafiltration from wastewaters, Desalination, 207 (2007) 125–133.

[12] J.S. Kim, C.H. Lee, S.H. Han, M.Y. Suh, Studies on complexation and solvent extraction of lanthanides in the presence of diaza-18-crown-6-di-isopropionic acid, Talanta, 45 (1997) 437–444.

[13] D. Mohan, S. Chander, Single component and multi-component adsorption of metal ions by activated carbons, Colloids Surf., A, 177 (2001) 183–196.

[14] Z. Reddad, C. Gerente, Y. Andres, P. Le Cloirec, Adsorption of several metal ions onto a low-cost biosorbent: kinetic and equilibrium studies, Environ. Sci. Technol., 36 (2002) 2067–2073.

[15] N. Ünlü, M. Ersoz, Adsorption characteristics of heavy metal ions onto a low cost biopolymeric sorbent from aqueous solutions, J. Hazard. Mater., 136 (2006) 272–280.

[16] S. Sen Gupta, K.G. Bhattacharyya, Kinetics of adsorption of metal ions on inorganic materials: a review, Adv. Colloids Interface Sci., 162 (2011) 39–58.

[17] V.K. Gupta, S. Sharma, Removal of zinc from aqueous solutions using bagasse fly ash − a low cost adsorbent, Ind. Eng. Chem. Res., 42 (2003) 6619–6624.

[18] K. Kadirvelu, K. Thamaraiselvi, C. Namasivayam, Removal of heavy metals from industrial wastewaters by adsorption onto activated carbon prepared from an agricultural solid waste, Bioresour. Technol., 76 (2001) 63–65.

[19] B. Subotić, J. Bronić, Removal of cerium(III) species from solutions using granulated zeolites, J. Radioanal. Nucl. Chem., 102 (1986) 465–481.

[20] E. Erdem, N. Karapinar, R. Donat, The removal of heavy metal cations by natural zeolites, J. Colloid Interface Sci., 280 (2004) 309–314.

[21] J.C.Y. Ng, W.H. Cheung, G. McKay, Equilibrium studies of the sorption of Cu(II) ions onto chitosan, J. Colloid Interface Sci., 255 (2002) 64–74.

[22] A.L. Taka, E. Fosso-Kankeu, K. Pillay, X.Y. Mbianda, Removal of cobalt and lead ions from wastewater samples using an insoluble nanosponge biopolymer composite: adsorption isotherm, kinetic, thermodynamic, and regeneration studies, Environ. Sci. Pollut. Res., 25 (2018) 21752–21767.

[23] R. Celis, M.C. HermosÍn, J. Cornejo, Heavy metal adsorption by functionalized clays, Environ. Sci. Technol., 34 (2000) 4593–4599.

[24] D. Sud, G. Mahajan, M.P. Kaur, Agricultural waste material as potential adsorbent for sequestering heavy metal ions from aqueous solutions − a review, Bioresour. Technol., 99 (2008) 6017–6027.

[25] M. Hua, S. Zhang, B. Pan, W. Zhang, L. Lv, Q. Zhang, Heavy metal removal from water/wastewater by nanosized metal oxides: a review, J. Hazard. Mater., 211–212 (2012) 317–331.

[26] M.I. Khan, S. Zafar, M.F. Azhar, A.R. Buzdar, W. Hassan, A. Aziz, M. Khraisheh, Leaves powder of syzgium cumini as an adsorbent for removal of congo red dye from aqueous solution, Fresenius Environ. Bull., 27 (2018) 3342–3350.

[27] M.I. Khan, S. Zafar, A.R. Buzdar, M.F. Azhar, W. Hassan, A. Aziz, Use of citrus sinensis leaves as a bioadsorbent for removal of congo red dye from aqueous solution, Fresenius Environ. Bull., 27 (2018) 4679–4688.

[28] M.I. Khan, S. Zafar, M.A. Khan, F. Mumtaz, P. Prapamonthon, A.R. Buzdar, Bougainvillea glabra leaves for adsorption of congo red from wastewater, Fresenius Environ. Bull., 27 (2018) 1456–1465.

[29] M.I. Khan, S. Zafar, H.B. Ahmad, M. Hussain, Z. Shafiq, Use of morus albal leaves as bioadsorbent for the removal of congo red dye, Fresenius Environ. Bull., 24 (2015) 2251–2258.

[30] M.I. Khan, M.A. Khan, S. Zafar, A.R. Buzdar, P. Prapamonthon, Adsorption kinetic, equilibrium and thermodynamic study for the removal of Congo Red from aqueous solution, Desal. Water Treat., 98 (2017) 294–305.

[31] M.I. Khan, L. Wu, A.N. Mondal, Z. Yao, L. Ge, T. Xu, Adsorption of methyl orange from aqueous solution on anion exchange membranes: adsorption kinetics and equilibrium, Membr. Water Treat., 7 (2016) 23–38.

[32] S. Zafar, M.I. Khan, M. Khraisheh, S. Shahida,T. Javed, M.L. Mirza, N. Khalid, Use of rice husk as an efective sorbent for the removal of cerium ions from aqueous solution: kinetic, equilibrium and thermodynamic studies, Desal. Water Treat., 150 (2019) 124–135.

[33] S. Zafar, M.I. Khan, M. Khraisheh, S. Shahida, N. Khalid, M.L. Mirza, Effective removal of lanthanum ions from aqueous solution using rice husk: impact of experimental variables, Desal. Water Treat., 132 (2019) 263–273.

[34] S. Zafar, M.I. Khan, M.H. Lashari, M. Khraisheh, F. Almomani, M.L. Mirza, N. Khalid, Removal of copper ions from aqueous solution using NaOH-treated rice husk, Emergent Mater., 3 (2020) 857–870.

[35] S. Zafar, M.I. Khan, M. Khraisheh, M.H. Lashari, S. Shahida, M.F. Azhar, P. Prapamonthon, M.L. Mirza, N. Khalid, Kinetic, equilibrium and thermodynamic studies for adsorption of nickel ions onto husk of *Oryza sativa*, Desal. Water Treat., 167 (2019) 277–290.

[36] S. Zafar, M.I. Khan, H. Rehman, J. Fernandez-Garcia, S. Shahida, P. Prapamonthon, M. Khraisheh, A. Rehman, H.B. Ahmad, M.L. Mirza, N. Khalid, M.H. Lashari, Kinetic, equilibrium, and thermodynamic studies for adsorptive removal of cobalt ions by rice husk from aqueous solution, Desal. Water Treat., 204 (2020) 285–296.

[37] M.A. Khan, M.I. Khan, S. Zafar, Removal of different anionic dyes from aqueous solution by anion exchange membrane, Membr. Water Treat., 8(2017) 259–277.

[38] M.I. Khan, S. Akhtar, S. Zafar, A. Shaheen, M.A. Khan, R. Luque, A. Rehman, Removal of Congo Red from aqueous solution by anion exchange membrane (EBTAC): adsorption kinetics and thermodynamics, Materials, 8 (2015) 4147–4161.

[39] M.I. Khan, T.M. Ansari, S. Zafar, A.R. Buzdar, M.A. Khan, F. Mumtaz, P. Prapamonthon, M. Akhtar, Acid green-25 removal from wastewater by anion exchange membrane: adsorption kinetic and thermodynamic studies, Membr. Water Treat., 9 (2018) 79–85.

[40] M.I. Khan, J. Su, L. Guo, Development of triethanolamine functionalized-anion exchange membrane for adsorptive removal of methyl orange from aqueous solution, Desal. Water Treat., 209 (2021) 342–352.

[41] S.K. Kazy, S. D'Souza, P. Sar, Uranium and thorium sequestration by a *Pseudomonas* sp.: mechanism and chemical characterization, J. Hazard. Mater., 163 (2009) 65–72.

[42] V.C. Srivastaa, I.D. Mall, I.M. Mishra, Characterization of mesoporous rice husk ash (RHA) and adsorption kinetics of metal ions from aqueous solution onto RHA, J. Hazard. Mater., 134 (2006) 257–267.

[43] S.K. Kazy, P. Sar, A.K. Sen, S.P. Singh, S.F. D'Souza, Extracellular polysaccha-rides of a copper sensitive and a copper resistant Pseudomonas aeruginosa stain: synthesis, chemical nature and copper binding, World J. Microbiol. Biotechnol., 18 (2002) 583–588.

[44] X. Ying-Mei, Q. Ji, H. De-Min, W. Dong-Mei, C. Hui-Ying, G. Jun, Z. Qiu-Min, Preparation of amorphous silica from oil shale residue and surface modification by silane coupling agent, Oil Shale, 27 (2010) 37–46.

[45] L. Ludueña, D. Fasce, V.A. Alvarez, P.M. Stefani, Nanocellulose from rice husk following alkaline treatment to remove silica, Bioresources, 6 (2011) 1440–1453.

[46] X. Zhang, X. Wang, Z. Chen, Radioactive Cobalt(II) removal from aqueous solutions using a reusable nanocomposite:

kinetic, isotherms, and mechanistic study, Int. J. Environ. Res. Public Health, 14 (2017) 1–19.

[47] B. Subramanyam, A. Das, Linearized and non-linearized isotherm models comparative study on adsorption of aqueous phenol solution in soil, Int. J. Environ. Sci. Technol., 6 (2009) 633–640.

[48] S. Kalyani, A. Krishnaiah, V.M. Boddu, Adsorption of divalent cobalt from aqueous solution onto chitosan–coated perlite beads as biosorbent, Sep. Sci. Technol., 42 (2007) 2767–2786.

[49] H. Parab, S. Joshi, M. Sudersanan, N. Shenoy, A. Lali, U. Sarma, Removal and recovery of cobalt from aqueous solutions by adsorption using low cost lignocellulosic biomass—coir pith, J. Environ. Sci. Health, Part A, 45 (2010) 603–611.

[50] W.K. Mekhemer, J.A. Hefne, N.M. Alandis, A. Aldayel, S. Al-Raddadi, Thermodynamic and kinetics of Co(II) adsorption onto natural and treated bentonite, Jordan J. Chem., 3 (2008) 409–423.

[51] K. Vijayaraghavan, K. Palanivelu, M. Velan, Biosorption of copper(II) and cobalt(II) from aqueous solutions by crab shell particles, Bioresour. Technol., 97 (2006) 1411–1419.

[52] K. Swayampakula, V.M. Boddu, S.K. Nadavala, K. Abburi, Competitive adsorption of Cu(II), Co(II) and Ni(II) from their binary and tertiary aqueous solutions using chitosan-coated perlite beads as biosorbent, J. Hazard. Mater., 170 (2009) 680–689.

[53] M.A.A. Munther Issa Kandah, H. Allaboun, Improvement of manure adsorption capacity for cobalt removal by chemical treatment with citric acid, Jordan J. Civil Eng., 2 (2008) 244–254.

[54] S. Dahiya, R.M. Tripathi, A.G. Hegde, Biosorption of heavy metals and radionuclide from aqueous solutions by pre-treated arca shell biomass, J. Hazard. Mater., 150 (2008) 376–386.

[55] K.K. Krishnani, X. Meng, C. Christodoulatos, V.M. Boddu, Biosorption mechanism of nine different heavy metals onto biomatrix from rice husk, J. Hazard. Mater., 153 (2008) 1222–1234.

[56] Ş. Kubilay, R. Gürkan, A. Savran, T. Şahan, Removal of Cu(II), Zn(II) and Co(II) ions from aqueous solutions by adsorption onto natural bentonite, Adsorption, 13 (2007) 41–51.

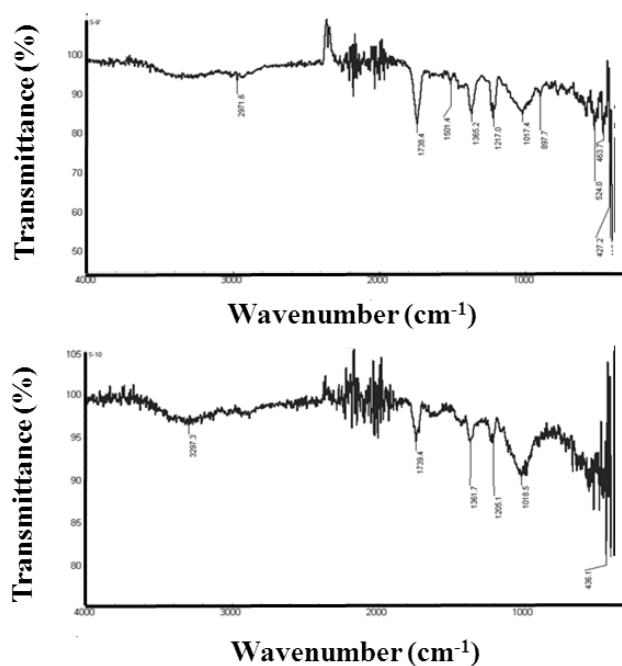## Supplementary information

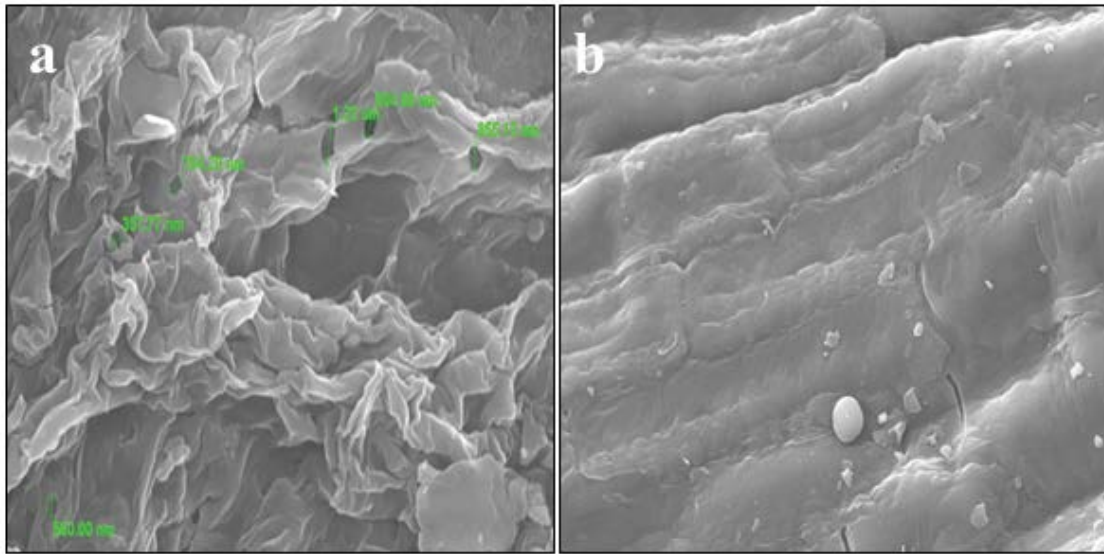Fig. S1. FTIR spectrum of (a) virgin TRH and (b) cobalt-loaded TRH.
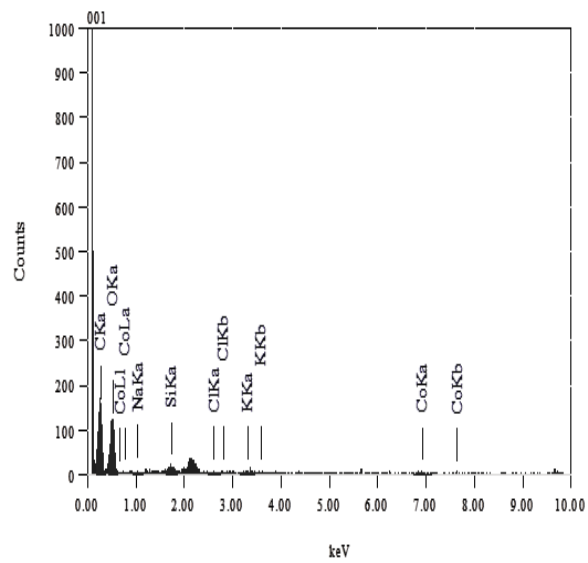
Fig. S2. SEM images of (a) virgin TRH and (b) cobalt-loaded TRH.

Fig. S3. EDX graph of Co(II) loaded TRH.